Cloud Chamber

Department of Physics, University of Toronto

Jace Alloway; alloway1 (1006940802)

Abstract

This work focuses on the investigation of the ionization of supersaturated ethyl alcohol vapour, an apparatus which is known as the 'cloud chamber'. The purpose of this experiment was to verify the optimal conditions for an 18 ± 1cm chamber and to determine the active depth of critical saturation crucial for observing particle tracks, which was approximately 2 ± 1cm in this experiment. This was done by moderating the amount of ethanol in the chamber and continuously monitoring the cooling applicant, which was liquid nitrogen, so that the results may be compared to a theoretical value of $2.2\pm$??cm. This work further investigates the measurement of background radiative phenomena, by which potential μ^- decay, β^- curling, and e^+e^- pair production could be seen. The application of a magnetic field via a magnet of 150 ± 10mT to charged background particles was investigated, and an analysis of the energy disposed into the chamber from Th-232 α^+ decays via the Bethe-Bloch equation was assessed and reconciled with an expected value of 4.01MeV.

Summary of Procedures, Analysis, and Results

A cloud chamber works by ionization. When charged particles pass through the critically-saturated part of the chamber, the surrounding air molecules are ionized. Since ethyl alcohol is a polar molecule, any ionized particle attracts the polar ethanol molecules until the ethanol begins to condense out of vapour. This becomes a visible drop, and thus tracks form when charged particles pass through the chamber.

The first task in operating the chamber was investigating the most optimal steps to constructing a maximized 'active region,' the first few centimeters of the chamber where particle tracks are detected. After investigating under- and over-saturated ethyl alcohol chambers (which proved to decrease the active region), it was found that about ~ 300mL of ethanol must be used to soak the felt, and ~ 50mL to coat the inside of the chamber walls, base, and glass lid. An over or under saturated chamber decreases the likelyhood of ethanol condensation and hence produces fewer tracks. The second step was to perform the first liquid nitrogen pour into the circular tin below the base plate, and this tin was filled up to the overflow hole. After 10-15 minutes, once the chamber began to cool, a second pour was taken out to the same overflow hole fill line. The chamber was then leveled, since an unleveled chamber draws tracks towards the lower basin of the base plate. This was done using a horizontal green laser mounted on the desk, and was levelled by rotating the screw stands holding up the chamber and sliding wooden risers underneath the legs. Any objects which needed to be placed in the chamber would be done so now. The LED was turned on to $V = 10.3 \pm 0.1V, I = 3.04 \pm 0.01A$ and the high-voltage BNC cable (and ground) would be attached and turned onto 3kV once any first tracks began to appear. The purpose of the HV cable was to increase ionization frequency by creating a potential difference between the glass lid and base plate, which would draw tracks down into the more active region of the chamber. See Figure 1 for photo of experimental setup. This was determined to be the most optimal set-up for the chamber operation, and was repeated twice. The temperature of the chamber was measured using a thermocouple, allowing one end to sit through the side port and the other through the top seal, ensuring both ends are resting on the surfaces.

The chamber height from base to lid was measured with a clear ruler (0.1cm-incremented) to be 18 ± 1cm, since sealant and acryllic cracks may have greatly altered the definiteness of the measurement. The active region of the chamber was measured to be 2 ± 1cm with the same ruler, again with large uncertainty due to temperature fluctations inside the chamber and visual limitations due to fogging. The notches in the base plate of the container, used for distance measurement

of tracks, was measured to be 10.0 ± 0.1cm between each, in horizontal and vertical directions. The active region of the chamber can be determined by finding the saturation function $S(z)$ and comparing it with a critical saturation S_{crit}, as defined by[1]

$$S(z) = \frac{z}{h}\left(1 - \frac{z}{h}\right)\Delta T^2\left[\frac{1}{2}\left(\frac{M_w L}{R\Delta T^2} - \frac{1}{\Delta T}\right)^2 - \frac{M_w L}{R\Delta T^3} + \frac{1}{2\Delta T^2}\right] \quad (1)$$

$$S_{\text{crit}} = \exp\left\{LM_w \frac{\Delta T(1 - z/h)}{RT_h^2}\right\} \quad (2)$$

where h is the chamber height (18 ± 1cm), L is the latent heat of vapourization (1048.4kJ/kg for ethanol; no uncertainty provided[3],[7]), M_w is the molecular weight (46.07 g/mol[4]), $R = 8.314$ J/mol is the gas constant, and $\Delta T = T_h - T_c$ is the temperature difference between the top and bottom of the chamber, measured with a thermocouple device to be $T_h = 276.6 \pm 0.1$ K, $T_c = 194.2 \pm 0.1$ K. When plotted in `matplotlib.pyplot`, the intersection of these curves was found using `scipy.optimize.brentq` and the critical saturation height for tracks, with these measurements, was found to be 2.2cm. Uncertainty was unable to be propagated due to time constraints, and no uncertainty function could be found for the complicated saturation expression for $S(z)$ or S_{crit}. However, since 2.2cm falls within the measured active region (2 ± 1cm), this was deemed sufficient until a proper uncertainty analysis could be completed. The comparison of these curves is shown in Figure 2.

The primary intent of this experiment was to observe pair production $\gamma\gamma \to e^+e^-$. Upon further reading, it was found that the minimum γ-ray energy requirement for pair production was 1.02MeV[2],[6], a relatively high photon energy for an undergraduate lab. Other sources[2] note that pair production probability could be increased by adding argon and iodine into the chamber, which was not present in the current lab. This was not further investigated. For background radiation, two scenarios were conducted: magnet absent in chamber, magnet present in chamber. The magnet, measured to be 150 ± 10mT, was propped in the center of the chamber with a wooden block of height 4.7 ± 0.1cm. This was done so that particles could pass around and underneath it so any possible curling would have been observed, however the overall field distributions and strength of the magnet could be improved for less-arbitrary field orientations (size doesn't matter, only aspect ratio does. Notebook pp.12). It was found that the magnet had minimal effects on charged particles, but curling was observed for some lower-energy electrons. Over many minutes of footage, many phenomena were observed: non-relativistic electron-electron nuclei scattering (Figure 3), β^- curling in the presence of a magnetic field (Figure 4), possible μ^- decay (into electron and anti-electron neutrino) (Figure 5), as well as presumed pair production (electron and positrons curl in opposite directions) (Figure 6).

The last task performed in this experiment was determining energy disposed into the chamber from the α^+ decay of Th-232. Th-232 was obtained and placed into the chamber with no magnet (when it was placed into the chamber with a magnet, minimal curling was observed). A 720px, 60FPS iPhone camera was used to record the alpha decays - ensuring that a set of four-notches was included in the frame so that distance measurements may be taken out. This was done in the Physlet Tracker application (see Figure 7), where an axes, grid, and calibration measurement were defined. Tracks were the measured in length and time to appear (number of frames), which could then determine the particle's velocity:

$$|v| = \ell \cdot \frac{n}{60} \quad (3)$$

where ℓ is the travelling distance of the particle and n is the number of traversed frames for the track to fully develop. These velocities were then included in the integrated Bethe-Bloch formula where the density correction $\frac{\delta}{2}$ was neglected[1],[8] since these energy deposits are must less than 1GeV. In atomic chemistry calculations (see notebook pp.9), the expected energy deposition should be approximately 4.01MeV from a Th-232 α^+ decay, thus neglecting the density term was deemed reasonable. The Bethe-Bloch formula becomes

$$E = -\rho K e^2 \frac{Z}{A\beta^2}\left[\log\frac{2m_e v^2}{I(1-\beta^2)} - \beta^2\right]\int_{x_1}^{x_2} dx \quad (4.1)$$

$$E = -\rho K e^2 \frac{Z}{A\beta^2}\left[\log\frac{2m_e v^2}{I(1-\beta^2)} - \beta^2\right]\ell \quad (4.2)$$

where ρ is the ethanol-saturated air density (0.038kg/m^3 [7](no error provided)), K is a constant

defined to be $K = 4\pi N_A r_e^2 m_e c^2 = 0.307075\text{MeV cm}^2/\text{g}$[1], Z is the mean atomic number (taken to be the mean sum of all atomic elements ethanol, carbon, oxygen, nitrogen, helium ≈ 14.8), A was taken to be the relative atomic number (15), thus $\frac{Z}{A} \approx 1$, and I the ionization energy $I = 10\text{eV} \cdot Z$. Lastly, $\beta = \frac{v}{c}$ is the relativistic correction. Upon analysis of the energy deposition distances, many notes were made on factors which affected the possible energy values (see notebook, pp26-29). Ultimately, it was found that most particles had an energy overestimate, and this was attributed to the particle velocity travelling under the timeframe specified by 1/60s, the 60FPS framerate in the footage. As most particle tracks just appeared in full form in the 1/60s timespan, it was determined that they must be travelling much faster than expected. Adjusting the frame number (in equation (3)) to a lower value, such as 0.1-0.3 frames (for the particle path to fully form), much more reasonable energies began appearing (see Table 1) on the expected order of $3 - 5$MeV. Energy uncertainties were calculated using the proportionality constant (multiplying ℓ) and the distance error $\delta\ell$. Many other observations were made on track measuring and formation, for which the lab notebook is referenced (pp. 29).

It is important to note some design improvements for the future of this experiment. As they are listed in the lab notebook (pp.17-21), but the summary here is that stronger radioactive sources (especially β^-) would make observing smaller tracks much easier to find. Acquiring a smaller magnet would allow for more definiteness of field line distributions and strengths instead of arbitrary orientation. Furthermore, the chamber height could be reduced so that magnetic effects may be observed without explicity placing the magnet in the chamber, only on the glass lid. Lastly, a simple improvement, is to increase notch density in the baseplate so any footage does not require a wide field of view for smaller measurements of particle tracks. If this experiment would be repeated, the focus would be more on determining uncertainties for the complicated functions (equations (1), (2)) and spending more time recording footage with a high-framerate or slow-motion camera (anything greater than 60FPS) and analyzing it accordingly.

To conclude, various experiments were conducted in the supersaturated chamber. The purpose of this experiment was to verify the optimal conditions for an 18 ± 1cm chamber and to determine the active depth of critical saturation crucial for observing particle tracks, which was approximately 2 ± 1cm as determined by measurement and $2.2 \pm ??$ as determined theoretically by equations (1) and (2). Further video footage observations found frequent molecular phenomena occuring in the chamber, including presumed muon decay and pair production, electron scattering and β^- curling, under the investigation of the application of a magnetic field. Th-232 α^+ decays were distance-measured and energy depositions were calculated using the Bethe-Bloch formula (4.2). At first, energy calculations appeared far too high, until it was speculated that particle velocities were much faster than determined, and this was adjusted (see Table 1). Photos, figures, and tables are located in Appendix I. Python code is an attached file. All other acquired data is in the lab notebook and as recorded footage.

Bibliography

[1] Clark, K. 2019. Cloud Chamber Lab Manual. University of Toronto, Physics.

[2] Simons, L. and Zuber, K., 1937. An investigation of the production of positive and negative electron pairs in a cloud chamber. Proceedings of the Royal Society of London. Series A-Mathematical and Physical Sciences, 159(898), pp.383-394.

[3] (Multiple Sources) P. J. Linstrom and W. G. Mallard. NIST Chemistry WebBook, NIST Standard Reference Database Number 69, ed., National Institute of Standards and Technology, Gaithersburg MD, 20899.

[4] (Multiple Sources) Cameo Chemicals, 1999. Ethyl Alcohol, Database.
`https://cameochemicals.noaa.gov/chris/EAL.pdf`

[5] Cloudylabs, 2008. Cloud chamber database, history, about.
`https://www.cloudylabs.fr/wp/les-processus-de-pertes-denergie-des-particules/`

[6] K. Buchtela, 2019. Radiochemical Methods — Gamma-Ray Spectrometry. Encyclopedia of Analytical Science (Third Edition), Academic Press, pp.15-22.

[7] (Multiple Sources) Thermal-Fluids Central. Ethanol.
`https://www.thermalfluidscentral.org/encyclopedia/index.php/Thermophysical_Properties:_Ethanol`

[8] Groom, D.E. and Klein, S.R., 2000. Passage of particles through matter. The European Physical Journal C-Particles and Fields, 15(1-4), pp.163-173.

Appendix I - Figures and Tables

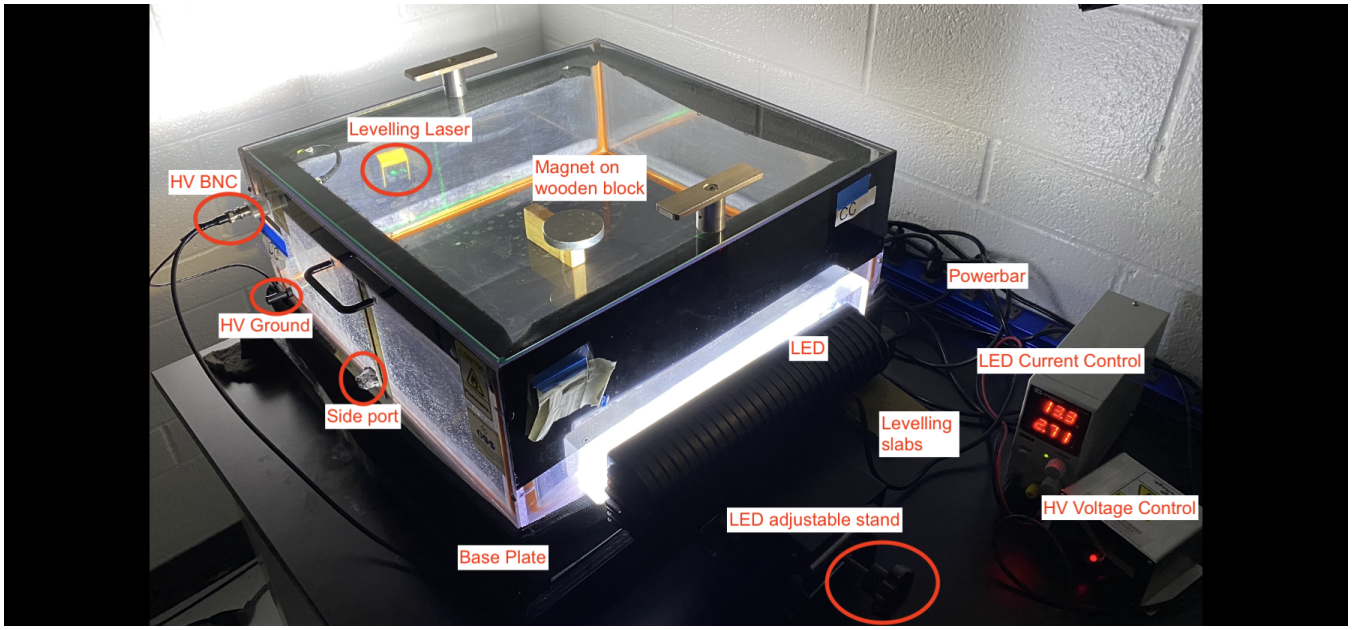

[Figure 1] Experimental setup. Note the magnet prop, LED, HV BNC and ground, laser level, and base plate.

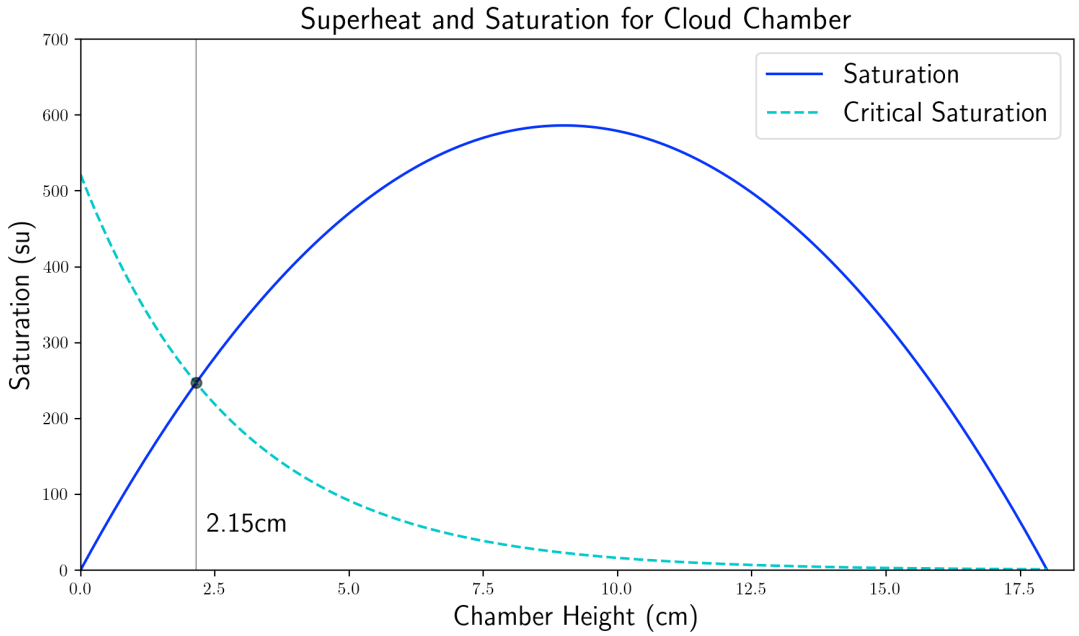

[Figure 2] Plot of critical saturation in the chamber. The active chamber region is defined for where $S_{\text{crit}} \geq S(z)$.

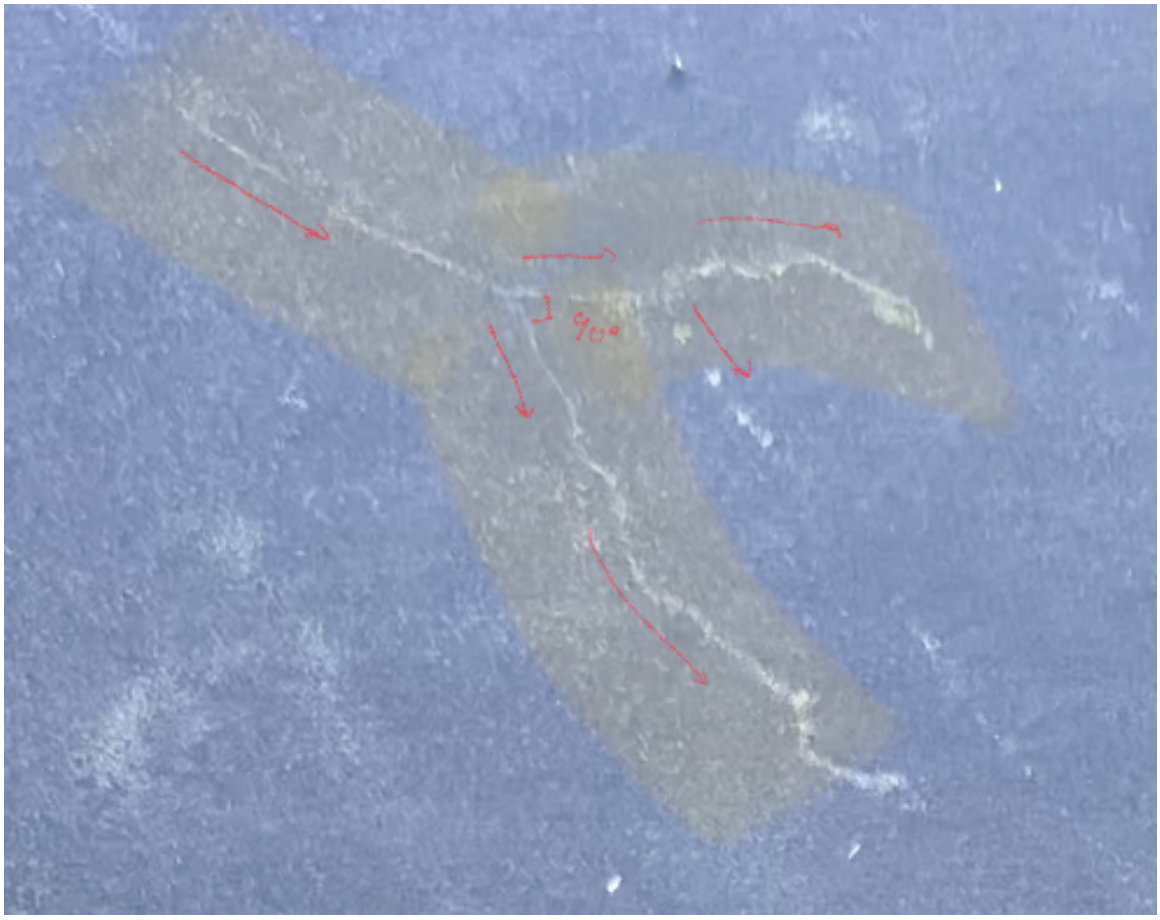

[Figure 3] Electron scattering off of bound electrons in nuclei[5] in the absence of a magnetic field. Red lines indicate direction of track.

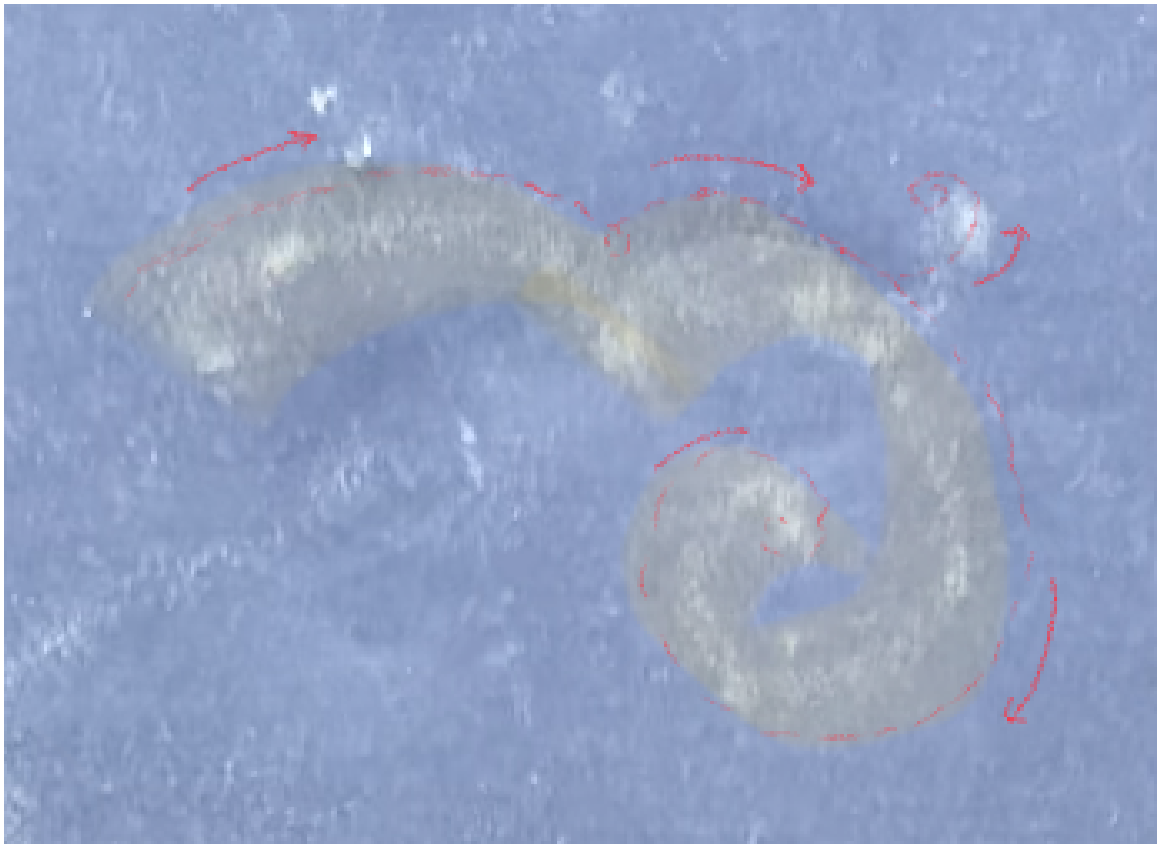

[Figure 4] Electron curling in the presence of the magnetic field (out of the page). Red lines indicate direction of track.

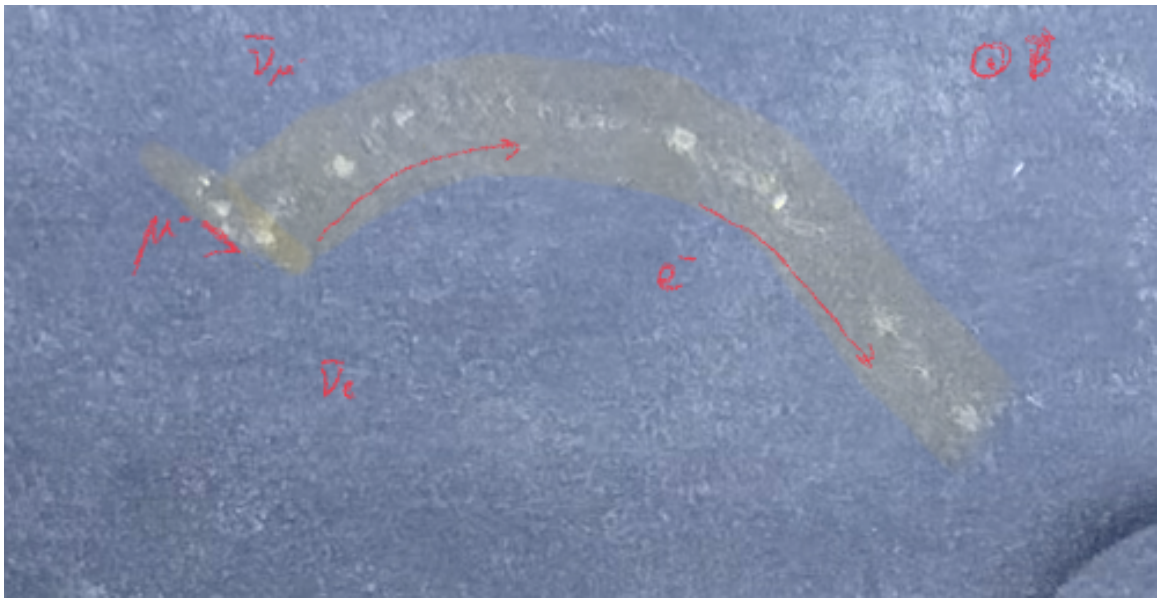

[Figure 5] Presumed decay of a muon. The short line indicates the short lifetime of the muon, while the curl indicates a scattered electron in the presence of the magnetic field out of the page. This could be mistaken for regular electron scattering, but is presumed to be muon decay when compared with other sources[5]. Red lines indicate direction of track.

[Figure 6] Presumed electron-positron pair production. While the magnetic field lines point out of the page, the lower particle curls opposite to the upper. The tracks originate out of nowhere, and continue from left to right as footage is played. Red lines indicate direction of track.

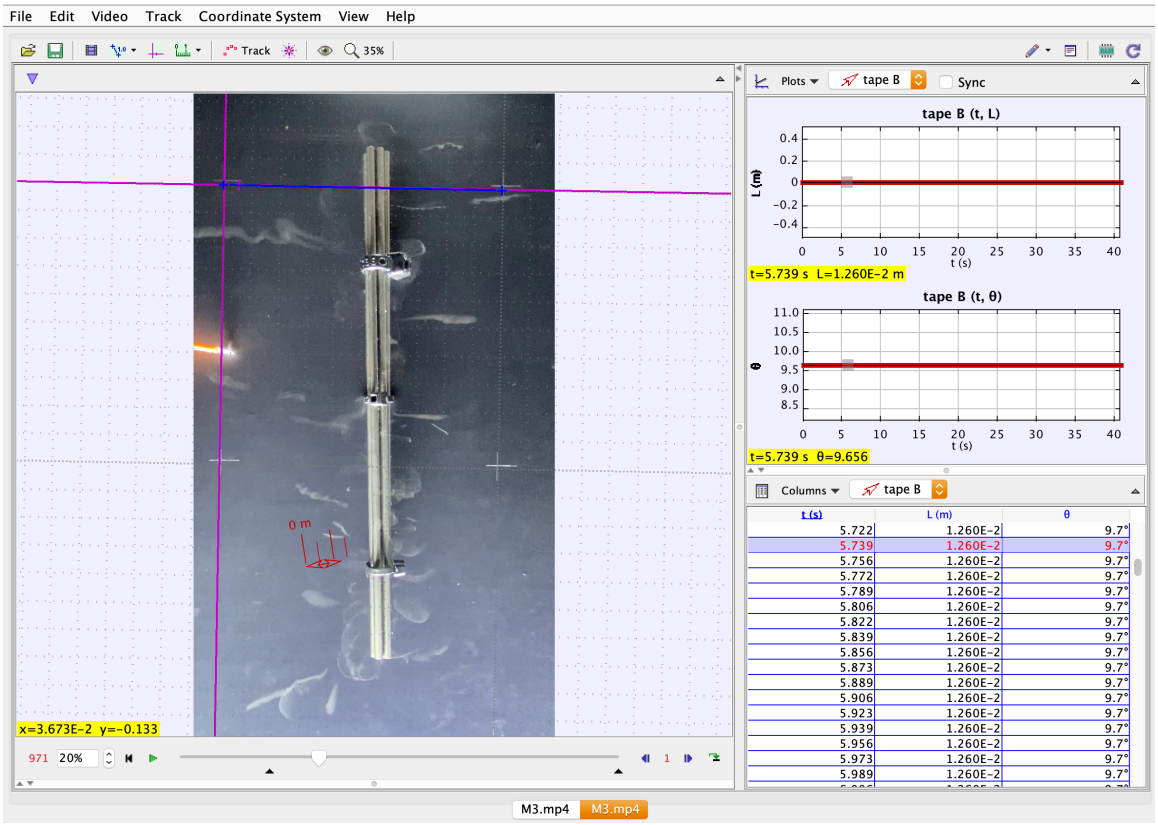

[Figure 7] Instance of particle distance measuring in Tracker app. The axis aligns with base plate notches, and the calibration stick is defined to be 0.10 ± 0.5m, although most error will be absorbed in systematic error due to the ruler measuring device. Particle tracks were measured by first identifying the frame where the track has first fully developed, then measuring tip-to-tail the length of the track.

Track No.	ℓ (cm)	$\delta\ell$ (cm)	Frame span	E (MeV)	δE (MeV)	Frame span, adjusted	E' (MeV)	$\delta E'$(MeV)
1	4.35	0.01	2	170	4	0.3	3.90	0.04
2	3.8	0.1	1	47	1	0.3	4.1	0.1
3	1.5	0.1	1	125	8	0.2	4.8	0.3
4	1.03	0.01	1	184	1	0.15	3.90	0.04
5	1.4	0.1	1	134	9	0.2	5.1	0.4
6	1.3	0.1	1	140	10	0.2	5.5	0.4

[Table 1] Energy deposition measurements from Th-232 α^+ decay, as measured in Tracker and analyzed in Python. Note that initially, larger framerates establish large energies above expected value, but adjusted framerates establish depositions within expected value. This could be attributed to framerate or a missing factor in the Bethe-Bloch formula, however the latter is unlikely.